Microglial TNFα controls synaptic $GABA_A$Rs, slow waves and memory consolidation during sleep

Maria Joana Pinto[1], Lucy Bizien[1], Julie M.J. Fabre[1], Nina Đukanović[1], Léa Cottin[1], Valentin Lepetz[1], Fiona Henderson[2], Marine Pujol[2], Romain W. Sala[1], Thibault Tarpin[1], Daniela Popa[1], Antoine Triller[1], Clément Léna[1*], Véronique Fabre[2*], Alain Bessis[1*]

Affiliations :

1-Institut de Biologie de l'École normale supérieure (IBENS), École normale supérieure, CNRS, INSERM, Université PSL, 75005 Paris, France.

2-Neurosciences Paris Seine - Institut de Biologie Paris Seine (NPS - IBPS), CNRS, INSERM, Sorbonne Universités, Paris, France

*Corresponding authors. Emails: alain.bessis@bio.ens.psl.eu; clement.lena@bio.ens.psl.eu; veronique.fabre@inserm.fr

Abstract: Microglia sense the changes in their environment. How microglia actively translate these changes into suitable cues to adapt brain physiology is unknown. We reveal an activity-dependent regulation of cortical inhibitory synapses by microglia, driven by purinergic signaling acting on P2RX7 and mediated by microglia-derived TNFα. We demonstrate that sleep induces microglia-dependent synaptic enrichment of $GABA_A$Rs in a manner dependent on microglial TNFα and P2RX7. We further show that microglia-specific depletion of TNFα alters slow waves during NREM sleep and blunts sleep-dependent memory consolidation. Together, our results reveal that microglia orchestrate sleep-intrinsic plasticity of synaptic $GABA_A$Rs, sculpt sleep slow waves and support sleep-dependent memory consolidation.

Microglia, the immune cells of the brain, tune neuronal networks in the healthy brain by finely modulating synapses[1]. They can sculpt developing circuits and remodel neuronal connectivity in adulthood by adjusting synapse density, function and plasticity[2–6]. Microglia accomplish these functions either by direct interaction with synaptic elements[5,7] or through the release of factors[4,8]. Many of the latter, such as prostaglandin, BDNF, IL-1β or TNFα, control synaptic plasticity and were independently shown to regulate sleep[9]. Recent work highlights the ability of microglia to control sleep duration[10,11]; however, whether and how microglia-released factors shape sleep via modulation of synaptic plasticity remains unknown.

Synapse plasticity in the sleeping brain likely supports crucial functions of sleep. In the cortex, spine turnover during sleep is associated to learning and memory[12,13] and, in parallel, wake-associated strengthening of excitatory synapses is downscaled during sleep[14,15]. Synaptic inhibition is critically involved in sleep generation and sleep oscillations[16–18] but whether and how inhibitory synapses are dynamically modulated during sleep remains poorly understood. Here, we uncover the molecular pathway underlying sleep-intrinsic microglia-dependent modulation of synaptic $GABA_AR$. Moreover, we demonstrate that microglial TNFα shapes sleep slow waves and supports sleep-dependent memory consolidation.

Daily modulation of $GABA_ARs$ in a sleep- and microglia-dependent manner

We first analyzed the modulation of synapses in the frontal cortex across the 24h light/dark cycle by measuring the synaptic content of neurotransmitter receptors (fig. 1 and fig. S1 and S2). Mice sleep more during the light phase and spend most of the dark phase awake. Therefore, we compared brains of mice at Zeitgeber time 18 (ZT18; dark/middle of wake phase) and at ZT6 (light/middle of sleep phase; fig. 1a). We focused on cortical layer 1 (L1) which is a key node for wide-scale cortical computation[19]. Consistent with the well-established downscaling of excitatory synapses during sleep[15], synaptic accumulation of the AMPA receptor subunit GluA2 was modestly but significantly decreased at ZT6 as compared to ZT18 (fig. S1). Of note, this level of change is comparable to previous analysis of daily changes in synaptic AMPARs[15,20]. Yet, analysis of L1 inhibitory synapses revealed an increased enrichment of synaptic, but not extra-synaptic, $GABA_AR$-γ2 and -α1 subunits at ZT6 (fig. 1a-c and fig. S2b-d), as well as an enhanced proportion of inhibitory synapses containing a $GABA_AR$ cluster (fig. S2e). No changes were observed in the total signal of $GABA_ARs$ (fig S2g), supportive of redistribution of the receptors rather than changes in expression. In contrast, in layer 5 (L5) the synaptic content of $GABA_ARγ2$ did not significantly differ between ZT6 and ZT18 (fig. 1e and fig. S2f). These results reveal a novel form of regulation of GABAergic synapses across the light/dark cycle with synaptic enrichment of $GABA_ARs$ in L1 during the light phase (ZT6), which likely contributes to upregulation of inhibitory transmission in the upper cortex during this phase[21].

To discriminate between a sleep-intrinsic or time of day-dependent regulation of synaptic $GABA_AR$, mice were forced to stay awake during their normal sleep period (sleep deprivation from ZT0 to ZT6, SD6; fig. 1a). The synaptic content of $GABA_AR$ was not different between mice at ZT18 and mice sleep-deprived in the light phase (SD6; fig. 1d), showing that modulation of synaptic $GABA_AR$ in L1 is driven by sleep-dependent mechanisms.

We have previously shown that microglia control the accumulation of receptors at inhibitory synapses in the spinal cord[22]. This prompted us to investigate the involvement of microglia in the modulation of synaptic $GABA_AR$ over the sleep/wake cycle. Strikingly, microglia depletion by feeding mice with the CSF1R antagonist PLX3397[23] (PLX; fig. S2a, b) completely prevented the changes in synaptic $GABA_ARs$ content between ZT6 and ZT18 (fig. 1c and fig. S2b,e). Importantly, as already shown[10] microglia depletion does not alter sleep during the light phase (fig S2h-I; table S1), discarding the possibility that lack of synaptic $GABA_ARs$ enrichment upon PLX3397 treatment results from perturbed sleep during the light phase. This shows that the sleep-dependent modulation of synaptic $GABA_AR$ in L1 requires microglia. Moreover, microglia depletion also abolished the reduction of synaptic AMPA receptor subunit GluA2 at ZT6 (fig S1), which agrees with the recent demonstration that light/dark changes in excitatory synaptic strength are microglia-dependent[10], a function that has been attributed to CX3CR1 signaling[10] and that was not further explored in this study.

Modulation of synaptic $GABA_AR$ by microglial P2RX7-TNFα signaling via CaMKII

We next sought to identify the molecular pathway underlying this novel microglia-dependent synaptic regulation. To accomplish so, we identified the molecular candidates regulating synaptic $GABA_ARs$ enrichment in an *ex vivo* paradigm of plasticity (fig. 2) and we subsequently validated these candidates *in vivo* (fig. 3). During sleep, excitatory synaptic plasticity is triggered by NMDAR-dependent dendritic calcium spikes in L1[13]. We thus selected an NMDA-induced GABAergic plasticity protocol, known as inhibitory long-term potentiation (iLTP). This form of plasticity, known to drive potentiation of excitatory synapses[24], also leads to an upregulation of synaptic $GABA_ARs$[25] in pyramidal neurons specifically at somatostatin interneurons inputs (SOM-IN)[26], which are mainly located in L1[27] (fig. S3). In agreement with the SOM-IN topographical organization, NMDA-induced iLTP in brain organotypic slices led to specific synaptic enrichment of $GABA_ARs$ in L1, but not in L5 somatic synapses (fig. 2a, b and fig. S4b-d). This protocol thus mimics *ex-vivo* the synaptic regulations occurring during the sleep/wake cycle, and we used it to identify the actors of the L1-restricted sleep-dependent synaptic enrichment of $GABA_ARs$ (fig. 1). We further demonstrated that this form of $GABA_AR$ plasticity was completely abolished when microglia were depleted by PLX (fig. 2a, b and fig. S4a, c). We ruled out possible secondary effects of PLX by showing the same effect upon microglia depletion using Mac1-Saporin (SAP) (fig. S4a) or inactivation using minocycline (fig. 2b).

Microglia produce a broad repertoire of signaling molecules that regulate synaptic function[1]. TNFα, which is mostly if not exclusively produced by microglia in the brain[28], controls basal synaptic strength[29], neurotransmitter receptors' dynamics and homeostatic synaptic plasticity[30]. We thus hypothesized that microglial TNFα controls the activity-dependent regulation of synaptic $GABA_AR$. Indeed, neutralization of TNFα by specific antibodies (fig. 2c) as well as conditional microglia-specific TNFα depletion (fig. 2d and fig. S5a) prevented the enrichment of synaptic $GABA_AR$ upon iLTP. Soluble TNFα derives from the cleavage of a membrane form of TNFα by the TNFα-converting enzyme (TACE)[31]. Both forms can signal through TNFR1 whereas TNFR2 is only activated by membrane TNFα[32]. The increase of synaptic

101 $GABA_A$Rs on iLTP-treated slices was prevented by TAPI-1, a TACE inhibitor, and by a TNFR1- but not by
102 a TNFR2-neutralizing antibody (fig. S5b). Finally, we showed that recombinant TNFα and activation of
103 TNFR1 were sufficient to increase synaptic accumulation of $GABA_A$Rα1 (fig. S5c-f). These experiments
104 show that microglial soluble TNFα acting through TNFR1 mediates the activity-dependent regulation of
105 $GABA_A$R in L1.
106 We next identified the signaling pathway between neuron and microglia leading to TNFα release upstream of
107 $GABA_A$Rs regulation. We first demonstrated that the well-established neuronal CX_3CL1-microglial CX_3CR1
108 signaling, with known roles in synaptic plasticity[33], is not involved (fig. S4e). Microglia behavior is finely
109 tuned by ATP via an array of purinergic receptors[34]. Microglial cells rapidly react to ATP following the
110 activation of neurons by glutamate and NMDA[35–37], and the stimulation of microglial P2RX7 promotes the
111 release of TNFα[38]. We thus investigated whether NMDA-induced release of ATP causes microglia-mediated
112 modulation of synaptic $GABA_A$R. Indeed, apyrase, a promoter of ATP hydrolysis, PPADS, a broad P2X
113 antagonist, or A740003, a specific P2RX7 antagonist, prevented the increase of synaptic $GABA_A$R upon
114 iLTP. In contrast, PSB0739 a specific inhibitor of P2RY12[39], had no effect on synaptic $GABA_A$R upon iLTP
115 suggesting that P2RY12 is not involved in this regulation (fig. 2e). Moreover, BzATP, a P2RX7 agonist[40]
116 was sufficient to increase postsynaptic $GABA_A$Rα1 in L1 (fig. 2f and fig. S6a,b) but not in L5 (fig. S6c). Of
117 note, BzATP had no effect when microglia were depleted or when TNFα was specifically inactivated in
118 microglia (fig. 2f). Thus, ATP/P2RX7 signaling acts upstream of microglial TNFα release to modulate
119 synaptic accumulation of $GABA_A$R.
120 Finally, we explored the intracellular signaling downstream of microglial TNFα. CaMKIIα is a
121 central neuronal mediator of postsynaptic plasticity whose activity is triggered by Ca^{2+}/calmodulin and can
122 be prolonged in a Ca^{2+}-independent manner by its autophosphorylation at Thr286[41]. Upon iLTP, Thr286-
123 autophosphorylated CaMKIIα leads to insertion of $GABA_A$Rs at synapses[42]. We reasoned that TNFα may
124 modulate CaMKIIα Thr286-phosphorylation, as observed in non-neuronal cells[43]. Indeed, Thr286-
125 phosphorylation of CaMKII was increased in L1 upon iLTP (fig. 2g) and this increase was abolished by
126 microglial depletion and by blocking P2RX7 or TNFα signaling (fig. 2h). In agreement, BzATP, which
127 upregulates the synaptic content of $GABA_A$Rs via a microglial relay, was sufficient to enhance CaMKII
128 Thr286-phosphorylation (fig. 2g, h). The finding that CaMKII Thr286 phosphorylation, and therefore its
129 activity, is gated by microglial TNFα downstream neuronal activity emphasizes a cardinal position of
130 microglia in fine-tuning synapses.
131 Collectively, our results support a bidirectional neuron-microglia crosstalk underlying activity-driven
132 GABAergic potentiation in L1 (fig. 2i): ATP released downstream neuronal activity activates microglial
133 P2RX7 with concomitant release of TNFα which modulates CaMKII autophosphorylation and thereby
134 enrichment of synaptic $GABA_A$Rs.
135
136 **Sleep-dependent modulation of synaptic $GABA_A$R driven by P2RX7 and microglial TNFα**
137 Having shown that microglial P2RX7/TNFα pathway controls L1 activity-dependent $GABA_A$R
138 plasticity via CaMKII autophosphorylation *ex-vivo*, we examined the involvement of this pathway in sleep-

139 dependent modulation of synaptic $GABA_AR$ across the light/dark cycle (fig. 1). We first showed that
140 CaMKII Thr286-phosphorylation, but not total CaMKII levels, was increased in L1 at ZT6 (fig. 3a, b and
141 fig. S7a). Notably, such regulation was not found in L5 (fig. S7b). Next, we showed that Thr286-
142 phosphorylation of CaMKII, as well as the synaptic content of $GABA_ARs$ in L1, were not enhanced at ZT6
143 in mice with microglia-specific TNFα depletion (micTNFα-KO, fig. S5a) and in P2rx7-KO mice (fig. 3a-c
144 and fig. S7c, d). This shows that P2RX7 and microglial TNFα drive daily fluctuations in CaMKII Thr286-
145 phosphorylation and are required for sleep-dependent $GABA_AR$ synaptic upregulation in L1 during the light
146 phase.
147
148 **NREM slow waves shaped by microglial TNFα**
149 The results above show that microglial TNFα is required for a novel sleep-dependent regulation of inhibitory
150 synapses in cortical L1. Sleep is an alternation of REM and NREM sleep periods which are hallmarked by
151 major EEG oscillatory patterns[44]. During NREM sleep, slow waves in the delta frequency band (0.1-4Hz),
152 quantified as slow wave activity (SWA), result from the synchronous alternation of active (up) and silent
153 (down) states of cortical neurons. Cortical GABAergic inhibition is a major actor of NREM sleep slow
154 waves[45,46]. In particular, the activation of somatostatin positive interneurons, that mainly target L1, triggers
155 down-states[17,18]. Because microglial TNFα modulates synaptic $GABA_AR$ at L1 during sleep, we anticipated
156 that it could also shape SWA. Sleep was analyzed using EMG and epidural EEG recordings, and we
157 concentrated our analysis in the frontal cortex where slow waves are predominant[47]. We first showed that
158 microglial TNFα has limited effects on sleep-wake patterns as shown by the lack of major alterations in the
159 amounts of wake, NREM and REM sleep between micTNFα-KO and tCTL mice along a light/dark cycle
160 (fig. 4a). Of note, the daily amount of REM sleep and number of REM bouts was increased on micTNFα-KO
161 (table S1). This phenotype agrees with a suppressive effect of TNFα on REM sleep when injected into the
162 basal forebrain[48]. We thus anticipate that microglial TNFα may control REM by acting at the basal forebrain,
163 which is out of the scope of this study and therefore not further explored.
164 We then analysed the spectral density of the EEG during sleep (figure 4b). In agreement with a role of
165 microglial TNFα in the regulation of SWA, we found a shift in the EEG spectral density towards lower
166 frequency activity during NREM sleep with a slower peak frequency in the delta range in micTNFα-KO as
167 compared to tCTL ($p=0.02539$), with no change in the delta power (Wilcoxon test: $W = 67$, $p=0.06$). There
168 were no detectable differences in the other frequency ranges nor in REM sleep (fig. 4b). Finally, we explored
169 how microglial TNFα shapes the properties of individual slow waves during NREM sleep. Slow waves were
170 identified in the epidural EEG as alternation of large transient negative and positive deflections in the 0.1-4
171 Hz filtered EEG (fig. 4c). We verified that these deflections correspond to up and down states respectively
172 (fig. S8; Nir et al. 2011). Remarkably, the maximum ascending slope of the slow waves, which coincides
173 with the onset of the cortical positive deflection (downstate; fig. S8c), was decreased and the duration of the
174 SW down state (fig. S8a, b) was increased in mice depleted of microglial TNFα as compared to controls (fig.
175 4d). These results indicate that microglial TNFα shapes slow waves during NREM sleep by favouring
176 transition into the down states.

Microglial TNFα tunes sleep-dependent memory consolidation.

Slow waves are known to play a causal role for the consolidation of memory during sleep[49,50]. Our previous results show that microglial TNFα exquisitely shapes slow waves during NREM sleep, leading us to anticipate a crucial role of microglial TNFα in the memory consolidation processes during sleep. To test this hypothesis, we compared the consolidation of different learning tasks known to be sleep-dependent[51–53] in micTNFα-KO and tCTL mice. In a first learning paradigm[51], mice learnt to run on top of a complex wheel attached to an accelerating rotarod in a first 20-trial session (S1). After one day of ad libitum sleep, performance on the complex wheel was assessed on a second 20-trial session by measuring the latency to fall (S2; fig. 5a, b).

We first confirmed that the learning, evaluated as the improvement of performance within each session, was not different between tCTL and micTNFα-KO (fig. 5c). This shows that lack of microglial TNFα did not alter complex motor learning, which is known to be sleep-independent[51]. We further showed that it does not impair locomotor activity and does not induce anxiety-like behavior as assessed in an open-field task (fig. S9). We next measured the improvement of performance <u>in the complex motor learning task</u> between S1 and S2 and found that it was higher in tCTL as compared with micTNFα-KO (fig. 5d). Finally, we tested the memory consolidation by comparing performance at the beginning of the second session (First S2) with either the last or the mean performance of the first session (Last S1 or Mean S1). In agreement with our initial hypothesis, memory consolidation was impaired in mice lacking microglial TNFα as compared to controls (fig. 5e). Remarkably, in this complex motor learning task, the improvement of performance between sessions and the memory consolidation are both known to be sleep-dependent processes[51]. To confirm the involvement of microglial TNFα in sleep-dependent memory consolidation, tCTL and micTNFα-KO mice performed a floor-texture recognition task, which is known to depend on cortex[52]. Mice first explored an arena with a single floor-texture (training session, smooth or rough) and containing two identical objects on each side. After one day of ad libitum sleep, mice explored the same arena containing the same two objects which were placed either on a familiar or on a novel floor-texture (testing session, smooth and rough). As expected[52], tCTL mice spent more time exploring the object located on the novel floor-texture during the testing session (fig 5f). In contrast, micTNFα-KO mice explored significantly less the object located on the novel floor-texture (fig 5f,g) confirming the impairment of memory consolidation on these mice.

Finally, tCTL and micTNFα-KO mice were tested in the novel-object recognition task (fig 5h, i). During the sampling session, mice explored two identical objects, and the next day (testing session) one of the original objects is replaced by a novel object. The amount of time taken to explore the novel object during the testing session provides a quantification of memory consolidation. Noteworthy, however, both genotypes exhibited larger amount of time spent exploring the novel object (fig 5i) indicating normal consolidation for this test.

Discussion

Microglia, the principal immune cells of the brain, are now acknowledged as instrumental for the perception of the external environment[54]. How microglia actively translate their external sensing into suitable cues to adapt circuitries in the healthy brain is yet unknown. Our results favour a model in which microglia sense neuronal activity through an ATP/P2RX7 signalling pathway and respond to it by releasing TNFα. Microglial TNFα then gates the phosphorylation of neuronal CaMKII that modulates $GABA_AR$ content at cortical synapses (fig. 2). During sleep, microglia act through TNFα to upregulate synaptic $GABA_AR$ content in L1 (figs. 1 and 3), which likely contributes to the strengthening of inhibitory transmission in the upper cortex[21]. In line with a prominent role of inhibition in the generation of slow waves[17,18,45,46,55] microglial TNFα shapes slow waves by controlling transition into down states (fig. 4). We finally demonstrate that microglial TNFα is determinant for sleep-dependent memory consolidation (fig. 5).

TNFα has long been known as a sleep factor. Administration of exogeneous TNFα promotes SWA and NREM sleep[56,57] whereas inhibition of endogenous TNFα reduces NREM sleep[refs in 58]. This is in apparent contradiction with our results showing no difference in NREM sleep amount in mice with microglia-specific TNFα depletion. Yet, to increase NREM sleep, TNFα was injected either directly in the brain[57] or intraperitoneally[56] at concentrations probably higher than the physiological concentration[59], with putative widespread diffusion and off-target and indirect effects. The studies using TNFα knock-out have not used cell specific and inducible inactivation and it is thus difficult to discriminate between microglial specific effect to indirect effects due to non-microglial TNFα and/or secondary developmental alterations. Finally, TNFα is also a major mediator of inflammation, which induces sleep dysfunction by yet elusive mechanisms[60]. Our work now provides possible molecular and cellular links between sleep and inflammation.

Our results were obtained from experiments performed both *in vivo* and in organotypic slices. The latter system closely mimics the *in vivo* brain by preserving tissue architecture and cellular composition. In these slices microglia retain their 3D ramified morphology and their functional properties[61–63]. They further conserve their ability to regulate synapses[22,64]. This indicates that functional interactions between neurons and microglia are conserved in organotypic slices. Indeed, in this work, we have identified microglial TNFα, ATP/P2RX7 and CaMKII as molecular actors of synaptic $GABA_ARs$ regulation in organotypic slices and we have further confirmed their role *in vivo* in the regulation of $GABA_ARs$ plasticity during the sleep/wake cycle.

Excitatory synapses are scaled down during sleep, through removal of AMPA receptors, to compensate for potentiation due to ongoing learning during wake[14]. Microglia contribute to downscaling during sleep by eliminating excitatory synapses[65], a behaviour presumably tuned down during wake by noradrenaline[66,67]. More recently, microglial CX3CR1 signalling was shown to differentially regulate excitatory synaptic transmission along the light/dark cycle[10]. We now show that microglia tune a sleep/wake regulation of inhibitory synapses restricted to cortical layer 1, via mobilization of the P2RX7/TNFα signalling and regulation of synaptic $GABA_AR$ content. Noteworthy, a comparable amplitude of changes in the $GABA_AR$

251 was found in the sleep/wake cycle analysis of the proteome of forebrain synaptosomes[20]. Altogether,
252 microglia are arising as active players in excitatory and inhibitory synapse remodelling along the sleep/wake
253 cycle, likely to underlie daily oscillations in synaptic strength[21,68,69].

254 Our study reveals that microglia can target specific sets of synapses by acting locally during sleep
255 time; however, the mechanisms supporting this spatiotemporal specificity have remained elusive. Microglia
256 expression of TNFα mRNA peaks at the middle of the light phase[70], when sleep is maximal. Specificity
257 could be achieved by differential microglial production of TNFα; however, our attempt to visualize
258 distribution of TNFα protein in the cortex at sleep and wake states failed due to unreliability of anti-TNFα
259 antibodies (not shown). Dynamics of TNFα release by microglia along a light/dark cycle in specific sleep
260 states thus awaits the advent of suitable tools. Another potential source of specificity may come from sleep-
261 specific patterns of neuronal activity and downstream ATP release that can then engage local microglia. For
262 instance, intense calcium spikes occur during sleep on the apical dendrites of pyramidal neurons inducing
263 plasticity in upper cortical layers[13]. ATP levels in frontal cortex actually peak in the light period in a sleep-
264 dependent manner[71]. Resolving the mechanism promoting spatiotemporal specificity of microglia functions
265 during sleep would give great insight into microglia-neuronal crosstalk in the physiological brain.

266 Cortical inhibition is involved in the control of slow wave activity during NREM sleep[17,55,72], with a
267 prominent role in the onset of down states[46,73]. Such control is likely achieved through inhibitory networks in
268 the upper layers of the cortex. Thalamic drive onto L1 inhibitory neurogliaform cells induces transition into
269 down states[45]. In addition, SOM-IN densely target layer 1 and their firing precedes entry into down states[18].
270 Accordingly SOM-IN stimulation increases the slope of slow waves and triggers down-states[17]. We now
271 show that in agreement with their ability to modulate inhibitory synapses in cortical L1, yet without ruling
272 out their possible involvement in other brain regions, microglia are possible regulators of slow waves during
273 NREM sleep through TNFα. Cortical inhibition also controls sleep-dependent memory consolidation[72],
274 which itself critically depends on slow waves[49,50]. It has even been proposed that one of the major
275 physiological role of sleep is to allow memory consolidation[74]. We now show that mice lacking microglial
276 TNFα display impaired sleep-dependent memory consolidation when tested in a complex rotator motor
277 learning task or in the floor-texture recognition (FTR) task, but not in the novel object recognition (NOR)
278 task. Strikingly, these later phenotypes mimicked that of mice lacking nNOS specifically in SOM-IN that
279 also display altered performance in FTR but not in NOR. This congruence strengthens the hypothesis that
280 microglial TNFα is a major actor of the regulation of cortical inhibition. Together with evidence of astrocytic
281 involvement in slow wave activity[75,76], our work offers insight into how local glial modulation of neuronal
282 networks may tune brain oscillations during sleep.

283 Finally, this work adds to the yet limited knowledge of microglia functions in the healthy adult
284 brain[4,6] and establishes microglia as genuine regulators of inhibitory synapses, brain oscillations and memory
285 in the healthy brain. Noteworthy, microglial regulation likely occurs through the control of CaMKIIα, which
286 is a cardinal regulator of synaptic plasticity[41]. It occurs on SOM-IN inputs, which are involved in the control
287 of complex behaviours such as sleep, but also decision making and learning[77]. Finally, this work

demonstrates that microglia tune slow waves and support memory consolidation during sleep[74]. We thus anticipate a far wider involvement of microglia in other forms of plasticity and higher brain functions.

References

1. Kettenmann, H., Kirchhoff, F., and Verkhratsky, A. (2013). Microglia: new roles for the synaptic stripper. Neuron *77*, 10–18. 10.1016/j.neuron.2012.12.023.
2. Favuzzi, E., Huang, S., Saldi, G.A., Binan, L., Ibrahim, L.A., Fernández-Otero, M., Cao, Y., Zeine, A., Sefah, A., Zheng, K., et al. (2021). GABA-receptive microglia selectively sculpt developing inhibitory circuits. Cell *184*, 4048-4063.e32. 10.1016/j.cell.2021.06.018.
3. Nguyen, P.T., Dorman, L.C., Pan, S., Vainchtein, I.D., Han, R.T., Nakao-Inoue, H., Taloma, S.E., Barron, J.J., Molofsky, A.B., Kheirbek, M.A., et al. (2020). Microglial Remodeling of the Extracellular Matrix Promotes Synapse Plasticity. Cell *182*, 388-403.e15. 10.1016/j.cell.2020.05.050.
4. Parkhurst, C.N., Yang, G., Ninan, I., Savas, J.N., Yates, J.R., Lafaille, J.J., Hempstead, B.L., Littman, D.R., and Gan, W.-B. (2013). Microglia promote learning-dependent synapse formation through brain-derived neurotrophic factor. Cell *155*, 1596–1609. 10.1016/j.cell.2013.11.030.
5. Schafer, D., Lehrman, E., Kautzman, A., Koyama, R., Mardinly, A., Yamasaki, R., Ransohoff, R., Greenberg, M., Barres, B., and Stevens, B. (2012). Microglia sculpt postnatal neural circuits in an activity and complement-dependent manner. Neuron *74*, 691–705. 10.1016/j.neuron.2012.03.026.
6. Wang, C., Yue, H., Hu, Z., Shen, Y., Ma, J., Li, J., Wang, X.-D., Wang, L., Sun, B., Shi, P., et al. (2020). Microglia mediate forgetting via complement-dependent synaptic elimination. Science *367*, 688–694. 10.1126/science.aaz2288.
7. Miyamoto, A., Wake, H., Ishikawa, A.W., Eto, K., Shibata, K., Murakoshi, H., Koizumi, S., Moorhouse, A.J., Yoshimura, Y., and Nabekura, J. (2016). Microglia contact induces synapse formation in developing somatosensory cortex. Nat. Commun. *7*, 12540. 10.1038/ncomms12540.
8. Lewitus, G.M., Konefal, S.C., Greenhalgh, A.D., Pribiag, H., Augereau, K., and Stellwagen, D. (2016). Microglial TNF-α Suppresses Cocaine-Induced Plasticity and Behavioral Sensitization. Neuron *90*, 483–491. 10.1016/j.neuron.2016.03.030.
9. Porkka-Heiskanen, T. (2013). Sleep homeostasis. Curr. Opin. Neurobiol. *23*, 799–805. 10.1016/j.conb.2013.02.010.
10. Corsi, G., Picard, K., di Castro, M.A., Garofalo, S., Tucci, F., Chece, G., del Percio, C., Golia, M.T., Raspa, M., Scavizzi, F., et al. (2022). Microglia modulate hippocampal synaptic transmission and sleep duration along the light/dark cycle. Glia *70*, 89–105. 10.1002/glia.24090.
11. Liu, H., Wang, X., Chen, L., Chen, L., Tsirka, S.E., Ge, S., and Xiong, Q. (2021). Microglia modulate stable wakefulness via the thalamic reticular nucleus in mice. Nat. Commun. *12*, 4646. 10.1038/s41467-021-24915-x.
12. Yang, G., Lai, C.S.W., Cichon, J., Ma, L., Li, W., and Gan, W.-B. (2014). Sleep promotes branch-specific formation of dendritic spines after learning. Science *344*, 1173–1178. 10.1126/science.1249098.
13. Li, W., Ma, L., Yang, G., and Gan, W.-B. (2017). REM sleep selectively prunes and maintains new synapses in development and learning. Nat. Neurosci. *20*, 427–437. 10.1038/nn.4479.
14. Vyazovskiy, V. V, Cirelli, C., Pfister-Genskow, M., Faraguna, U., and Tononi, G. (2008). Molecular and electrophysiological evidence for net synaptic potentiation in wake and depression in sleep. Nat. Neurosci. *11*, 200–208. 10.1038/nn2035.
15. Diering, G.H., Nirujogi, R.S., Roth, R.H., Worley, P.F., Pandey, A., and Huganir, R.L. (2017). Homer1a drives homeostatic scaling-down of excitatory synapses during sleep. Science *355*, 511–515. 10.1126/science.aai8355.
16. Dixon, C.L., Harrison, N.L., Lynch, J.W., and Keramidas, A. (2015). Zolpidem and eszopiclone prime α1β2γ2 $GABA_A$ receptors for longer duration of activity. Br. J. Pharmacol. *172*, 3522–3536. 10.1111/bph.13142.
17. Funk, C.M., Peelman, K., Bellesi, M., Marshall, W., Cirelli, C., and Tononi, G. (2017). Role of somatostatin-positive cortical interneurons in the generation of sleep slow waves. J. Neurosci., 1303–1317. 10.1523/JNEUROSCI.1303-17.2017.
18. Niethard, N., Ngo, H.-V.V., Ehrlich, I., and Born, J. (2018). Cortical circuit activity underlying sleep slow oscillations and spindles. Proc. Natl. Acad. Sci. *115*, E9220–E9229. 10.1073/pnas.1805517115.
19. Schuman, B., Dellal, S., Prönneke, A., Machold, R., and Rudy, B. (2021). Neocortical Layer 1: An Elegant Solution to Top-Down and Bottom-Up Integration. Annu. Rev. Neurosci. 10.1146/annurev-neuro-100520-012117.

20. Noya, S.B., Colameo, D., Brüning, F., Spinnler, A., Mircsof, D., Opitz, L., Mann, M., Tyagarajan, S.K., Robles, M.S., and Brown, S.A. (2019). The forebrain synaptic transcriptome is organized by clocks but its proteome is driven by sleep. Science *366*, eaav2642. 10.1126/science.aav2642.
21. Bridi, M.C.D., Zong, F.-J., Min, X., Luo, N., Tran, T., Qiu, J., Severin, D., Zhang, X.-T., Wang, G., Zhu, Z.-J., et al. (2020). Daily Oscillation of the Excitation-Inhibition Balance in Visual Cortical Circuits. Neuron *105*, 621-629.e4. 10.1016/j.neuron.2019.11.011.
22. Cantaut-Belarif, Y., Antri, M., Pizzarelli, R., Colasse, S., Vaccari, I., Soares, S., Renner, M., Dallel, R., Triller, A., and Bessis, A. (2017). Microglia control the glycinergic but not the GABAergic synapses via prostaglandin E2 in the spinal cord. J. Cell Biol. *216*, 2979–2989. 10.1083/jcb.201607048.
23. Elmore, M.R.P., Najafi, A.R., Koike, M.A., Dagher, N.N., Spangenberg, E.E., Rice, R.A., Kitazawa, M., Matusow, B., Nguyen, H., West, B.L., et al. (2014). Colony-stimulating factor 1 receptor signaling is necessary for microglia viability, unmasking a microglia progenitor cell in the adult brain. Neuron *82*, 380–397. 10.1016/j.neuron.2014.02.040.
24. Lee, H.-K., Kameyama, K., Huganir, R.L., and Bear, M.F. (1998). NMDA Induces Long-Term Synaptic Depression and Dephosphorylation of the GluR1 Subunit of AMPA Receptors in Hippocampus. Neuron *21*, 1151–1162. 10.1016/S0896-6273(00)80632-7.
25. Petrini, E.M., Ravasenga, T., Hausrat, T.J., Iurilli, G., Olcese, U., Racine, V., Sibarita, J.-B., Jacob, T.C., Moss, S.J., Benfenati, F., et al. (2014). Synaptic recruitment of gephyrin regulates surface GABA(A) receptor dynamics for the expression of inhibitory LTP. Nat. Commun. *5*, 3921. 10.1038/ncomms4921.
26. Chiu, C.Q., Martenson, J.S., Yamazaki, M., Natsume, R., Sakimura, K., Tomita, S., Tavalin, S.J., and Higley, M.J. (2018). Input-Specific NMDAR-Dependent Potentiation of Dendritic GABAergic Inhibition. Neuron *97*, 368-377.e3. 10.1016/j.neuron.2017.12.032.
27. Tremblay, R., Lee, S., and Rudy, B. (2016). GABAergic Interneurons in the Neocortex: From Cellular Properties to Circuits. Neuron *91*, 260–292. 10.1016/j.neuron.2016.06.033.
28. Zeisel, A., Hochgerner, H., Lönnerberg, P., Johnsson, A., Memic, F., van der Zwan, J., Häring, M., Braun, E., Borm, L.E., La Manno, G., et al. (2018). Molecular Architecture of the Mouse Nervous System. Cell *174*, 999-1014.e22. 10.1016/j.cell.2018.06.021.
29. Santello, M., Bezzi, P., and Volterra, A. (2011). TNFα Controls Glutamatergic Gliotransmission in the Hippocampal Dentate Gyrus. Neuron *69*, 988–1001. 10.1016/j.neuron.2011.02.003.
30. Stellwagen, D., and Malenka, R.C. (2006). Synaptic scaling mediated by glial TNF-α. Nature *440*, 1054–1059. 10.1038/nature04671.
31. Black, R.A., Rauch, C.T., Kozlosky, C.J., Peschon, J.J., Slack, J.L., Wolfson, M.F., Castner, B.J., Stocking, K.L., Reddy, P., Srinivasan, S., et al. (1997). A metalloproteinase disintegrin that releases tumour-necrosis factor-alpha from cells. Nature *385*, 729–733. 10.1038/385729a0.
32. Holbrook, J., Lara-Reyna, S., Jarosz-Griffiths, H., and McDermott, M. (2019). Tumour necrosis factor signalling in health and disease [version 1; referees: 2 approved]. F1000Research *8*. 10.12688/f1000research.17023.1.
33. Rogers, J.T., Morganti, J.M., Bachstetter, A.D., Hudson, C.E., Peters, M.M., Grimmig, B. a., Weeber, E.J., Bickford, P.C., and Gemma, C. (2011). CX3CR1 Deficiency Leads to Impairment of Hippocampal Cognitive Function and Synaptic Plasticity. J. Neurosci. *31*, 16241–16250. 10.1523/JNEUROSCI.3667-11.2011.
34. Madry, C., and Attwell, D. (2015). Receptors, Ion Channels and Signaling Mechanisms Underlying Microglial Dynamics. J. Biol. Chem. 10.1074/jbc.R115.637157.
35. Li, Y., Du, X., Liu, C., Wen, Z., and Du, J. (2012). Reciprocal Regulation between Resting Microglial Dynamics and Neuronal Activity In Vivo. Dev. Cell *23*, 1189–1202. 10.1016/j.devcel.2012.10.027.
36. Dissing-Olesen, L., LeDue, J.M., Rungta, R.L., Hefendehl, J.K., Choi, H.B., and MacVicar, B.A. (2014). Activation of Neuronal NMDA Receptors Triggers Transient ATP-Mediated Microglial Process Outgrowth. J. Neurosci. *34*, 10511–10527. 10.1523/JNEUROSCI.0405-14.2014.
37. Badimon, A., Strasburger, H.J., Ayata, P., Chen, X., Nair, A., Ikegami, A., Hwang, P., Chan, A.T., Graves, S.M., Uweru, J.O., et al. (2020). Negative feedback control of neuronal activity by microglia. Nature *586*, 417–423. 10.1038/s41586-020-2777-8.
38. Suzuki, T., Hide, I., Ido, K., Kohsaka, S., Inoue, K., and Nakata, Y. (2004). Production and release of neuroprotective tumor necrosis factor by P2X7 receptor-activated microglia. J. Neurosci. Off. J. Soc. Neurosci. *24*, 1–7. 10.1523/JNEUROSCI.3792-03.2004.
39. Hoffmann, K., Baqi, Y., Morena, M.S., Glänzel, M., Müller, C.E., and von Kügelgen, I. (2009). Interaction of new, very potent non-nucleotide antagonists with Arg256 of the human platelet P2Y12

receptor. J. Pharmacol. Exp. Ther. *331*, 648–655. 10.1124/jpet.109.156687.
40. Surprenant, A., Rassendren, F., Kawashima, E., North, R.A., and Buell, G. (1996). The cytolytic P2Z receptor for extracellular ATP identified as a P2X receptor (P2X7). Science *272*, 735–738. 10.1126/science.272.5262.735.
41. Bayer, K.U., and Schulman, H. (2019). CaM Kinase: Still Inspiring at 40. Neuron *103*, 380–394. 10.1016/j.neuron.2019.05.033.
42. Marsden, K.C., Shemesh, A., Bayer, K.U., and Carroll, R.C. (2010). Selective translocation of Ca2+/calmodulin protein kinase IIα (CaMKIIα) to inhibitory synapses. Proc. Natl. Acad. Sci. U. S. A. *107*, 20559–20564. 10.1073/pnas.1010346107.
43. Defer, N., Azroyan, A., Pecker, F., and Pavoine, C. (2007). TNFR1 and TNFR2 signaling interplay in cardiac myocytes. J. Biol. Chem. *282*, 35564–35573. 10.1074/jbc.M704003200.
44. Adamantidis, A.R., Gutierrez Herrera, C., and Gent, T.C. (2019). Oscillating circuitries in the sleeping brain. Nat. Rev. Neurosci. *20*, 746–762. 10.1038/s41583-019-0223-4.
45. Hay, Y.A., Deperrois, N., Fuchsberger, T., Quarrell, T.M., Koerling, A.-L., and Paulsen, O. (2021). Thalamus mediates neocortical Down state transition via GABAB-receptor-targeting interneurons. Neuron *109*, 2682-2690.e5. 10.1016/j.neuron.2021.06.030.
46. Lemieux, M., Chauvette, S., and Timofeev, I. (2015). Neocortical inhibitory activities and long-range afferents contribute to the synchronous onset of silent states of the neocortical slow oscillation. J. Neurophysiol. *113*, 768–779. 10.1152/jn.00858.2013.
47. Vyazovskiy, V.V., Ruijgrok, G., Deboer, T., and Tobler, I. (2006). Running Wheel Accessibility Affects the Regional Electroencephalogram during Sleep in Mice. Cereb. Cortex *16*, 328–336. 10.1093/cercor/bhi110.
48. Terao, A., Matsumura, H., Yoneda, H., and Saito, M. (1998). Enhancement of slow-wave sleep by tumor necrosis factor-alpha is mediated by cyclooxygenase-2 in rats. Neuroreport *9*, 3791–3796. 10.1097/00001756-199812010-00005.
49. Fattinger, S., de Beukelaar, T.T., Ruddy, K.L., Volk, C., Heyse, N.C., Herbst, J.A., Hahnloser, R.H.R., Wenderoth, N., and Huber, R. (2017). Deep sleep maintains learning efficiency of the human brain. Nat. Commun. *8*, 15405. 10.1038/ncomms15405.
50. Marshall, L., Helgadóttir, H., Mölle, M., and Born, J. (2006). Boosting slow oscillations during sleep potentiates memory. Nature *444*, 610–613. 10.1038/nature05278.
51. Nagai, H., de Vivo, L., Bellesi, M., Ghilardi, M.F., Tononi, G., and Cirelli, C. (2017). Sleep Consolidates Motor Learning of Complex Movement Sequences in Mice. Sleep *40*. 10.1093/sleep/zsw059.
52. Miyamoto, D., Hirai, D., Fung, C.C.A., Inutsuka, A., Odagawa, M., Suzuki, T., Boehringer, R., Adaikkan, C., Matsubara, C., Matsuki, N., et al. (2016). Top-down cortical input during NREM sleep consolidates perceptual memory. Science *352*, 1315–1318. 10.1126/science.aaf0902.
53. Rolls, A., Colas, D., Adamantidis, A., Carter, M., Lanre-Amos, T., Heller, H.C., and de Lecea, L. (2011). Optogenetic disruption of sleep continuity impairs memory consolidation. Proc. Natl. Acad. Sci. U. S. A. *108*, 13305–13310. 10.1073/pnas.1015633108.
54. Thion, M.S., Ginhoux, F., and Garel, S. (2018). Microglia and early brain development: An intimate journey. Science *362*, 185–189. 10.1126/science.aat0474.
55. Zucca, S., D'Urso, G., Pasquale, V., Vecchia, D., Pica, G., Bovetti, S., Moretti, C., Varani, S., Molano-Mazón, M., Chiappalone, M., et al. (2017). An inhibitory gate for state transition in cortex. eLife *6*. 10.7554/eLife.26177.
56. Fang, J., Wang, Y., and Krueger, J.M. (1997). Mice lacking the TNF 55 kDa receptor fail to sleep more after TNFalpha treatment. J. Neurosci. Off. J. Soc. Neurosci. *17*, 5949–5955.
57. Yoshida, H., Peterfi, Z., García-García, F., Kirkpatrick, R., Yasuda, T., and Krueger, J.M. (2004). State-specific asymmetries in EEG slow wave activity induced by local application of TNFα. Brain Res. *1009*, 129–136. 10.1016/j.brainres.2004.02.055.
58. Rockstrom, M.D., Chen, L., Taishi, P., Nguyen, J.T., Gibbons, C.M., Veasey, S.C., and Krueger, J.M. (2018). Tumor necrosis factor alpha in sleep regulation. Sleep Med. Rev. *40*, 69–78. 10.1016/j.smrv.2017.10.005.
59. Garré, J.M., Silva, H.M., Lafaille, J.J., and Yang, G. (2017). CX3CR1+ monocytes modulate learning and learning-dependent dendritic spine remodeling via TNF-α. Nat. Med. *23*, 714–722. 10.1038/nm.4340.
60. Irwin, M.R. (2019). Sleep and inflammation: partners in sickness and in health. Nat. Rev. Immunol. 10.1038/s41577-019-0190-z.
61. De Simoni, A., Allen, N.J., and Attwell, D. (2008). Charge compensation for NADPH oxidase

activity in microglia in rat brain slices does not involve a proton current. Eur. J. Neurosci. *28*, 1146–1156. 10.1111/j.1460-9568.2008.06417.x.
62. Delbridge, A.R.D., Huh, D., Brickelmaier, M., Burns, J.C., Roberts, C., Challa, R., Raymond, N., Cullen, P., Carlile, T.M., Ennis, K.A., et al. (2020). Organotypic Brain Slice Culture Microglia Exhibit Molecular Similarity to Acutely-Isolated Adult Microglia and Provide a Platform to Study Neuroinflammation. Front. Cell. Neurosci. *14*, 592005. 10.3389/fncel.2020.592005.
63. Weinhard, L., di Bartolomei, G., Bolasco, G., Machado, P., Schieber, N.L., Neniskyte, U., Exiga, M., Vadisiute, A., Raggioli, A., Schertel, A., et al. (2018). Microglia remodel synapses by presynaptic trogocytosis and spine head filopodia induction. Nat. Commun. *9*. 10.1038/s41467-018-03566-5.
64. Pascual, O., Achour, S.B., Rostaing, P., Triller, A., and Bessis, A. (2012). Microglia activation triggers astrocyte-mediated modulation of excitatory neurotransmission. Proc Natl Acad Sci USA *109*, E197-205. 10.1073/pnas.1111098109.
65. Choudhury, M.E., Miyanishi, K., Takeda, H., Islam, A., Matsuoka, N., Kubo, M., Matsumoto, S., Kunieda, T., Nomoto, M., Yano, H., et al. (2019). Phagocytic elimination of synapses by microglia during sleep. Glia, 1–16. 10.1002/glia.23698.
66. Liu, Y.U., Ying, Y., Li, Y., Eyo, U.B., Chen, T., Zheng, J., Umpierre, A.D., Zhu, J., Bosco, D.B., Dong, H., et al. (2019). Neuronal network activity controls microglial process surveillance in awake mice via norepinephrine signaling. Nat. Neurosci. *22*, 1771–1781. 10.1038/s41593-019-0511-3.
67. Stowell, R.D., Sipe, G.O., Dawes, R.P., Batchelor, H.N., Lordy, K.A., Whitelaw, B.S., Stoessel, M.B., Bidlack, J.M., Brown, E., Sur, M., et al. (2019). Noradrenergic signaling in the wakeful state inhibits microglial surveillance and synaptic plasticity in the mouse visual cortex. Nat. Neurosci. *22*, 1782–1792. 10.1038/s41593-019-0514-0.
68. Tononi, G., and Cirelli, C. (2019). Sleep and synaptic down-selection. Eur. J. Neurosci. 10.1111/ejn.14335.
69. Vyazovskiy, V.V., Cirelli, C., Pfister-Genskow, M., Faraguna, U., and Tononi, G. (2008). Molecular and electrophysiological evidence for net synaptic potentiation in wake and depression in sleep. Nat. Neurosci. *11*, 200–208. 10.1038/nn2035.
70. Fonken, L.K., Frank, M.G., Kitt, M.M., Barrientos, R.M., Watkins, L.R., and Maier, S.F. (2015). Microglia inflammatory responses are controlled by an intrinsic circadian clock. Brain. Behav. Immun. *45*, 171–179. 10.1016/j.bbi.2014.11.009.
71. Dworak, M., McCarley, R.W., Kim, T., Kalinchuk, A. V., and Basheer, R. (2010). Sleep and brain energy levels: ATP changes during sleep. J. Neurosci. Off. J. Soc. Neurosci. *30*, 9007–9016. 10.1523/JNEUROSCI.1423-10.2010.
72. Zielinski, M.R., Atochin, D.N., McNally, J.M., McKenna, J.T., Huang, P.L., Strecker, R.E., and Gerashchenko, D. (2019). Somatostatin+/nNOS+ neurons are involved in delta electroencephalogram activity and cortical-dependent recognition memory. Sleep *42*. 10.1093/sleep/zsz143.
73. Chen, J.-Y., Chauvette, S., Skorheim, S., Timofeev, I., and Bazhenov, M. (2012). Interneuron-mediated inhibition synchronizes neuronal activity during slow oscillation. J. Physiol. *590*, 3987–4010. 10.1113/jphysiol.2012.227462.
74. Klinzing, J.G., Niethard, N., and Born, J. (2019). Mechanisms of systems memory consolidation during sleep. Nat. Neurosci. *22*, 1598–1610. 10.1038/s41593-019-0467-3.
75. Szabó, Z., Héja, L., Szalay, G., Kékesi, O., Füredi, A., Szebényi, K., Dobolyi, Á., Orbán, T.I., Kolacsek, O., Tompa, T., et al. (2017). Extensive astrocyte synchronization advances neuronal coupling in slow wave activity in vivo. Sci. Rep. *7*, 6018. 10.1038/s41598-017-06073-7.
76. Vaidyanathan, T.V., Collard, M., Yokoyama, S., Reitman, M.E., and Poskanzer, K.E. (2021). Cortical astrocytes independently regulate sleep depth and duration via separate GPCR pathways. eLife *10*, e63329. 10.7554/eLife.63329.
77. Adler, A., Zhao, R., Shin, M.E., Yasuda, R., and Gan, W.-B. (2019). Somatostatin-Expressing Interneurons Enable and Maintain Learning-Dependent Sequential Activation of Pyramidal Neurons. Neuron *102*, 202-216.e7. 10.1016/j.neuron.2019.01.036.

Acknowledgments:
This work was funded by : Agence nationale pour la recherche : SYNTRACK -R17096DJ (AT); Agence nationale pour la recherche: EXPECT 17-CE37-0022-2 (CL, DP); European Research Council : PLASTINHIB Project No: 322821 and MICROCOPS (AT); Human Brain Project : HBP SGA2-OPE-2018-0017 (AT); EMBO fellowship: ALTF 362-2017 (MJP);

We gratefully acknowledge Astou Tangara, Benjamin Mathieu and the IBENS imaging facility (IMACHEM-IBiSA), member of the French National Research Infrastructure France-BioImaging (ANR-10-INBS-04), which received support from the "Fédération pour la Recherche sur le Cerveau - Rotary International France" (2011) and from the program « Investissements d'Avenir » ANR-10-LABX-54 MEMOLIFE.

We are grateful to Amandine Delecourt, Eleonore Touzalin, Deborah Souchet for excellent technical assistance.

We thank Sonia Garel (IBENS, Paris), Etienne Audinat (Institut de génomique fonctionnelle, Montpellier) and Lauriane Ulmann and François Rassendren (Institut de génomique fonctionnelle, Montpellier) for providing $CX_3CR1^{CreERT2}$ and Ai9 ; TNF^{flox} and P2rx7 -KOs respectively.

We are grateful to the IBPS Animal facility for breeding and care, the IBPS-NPS Phenotypic core facility, and particularly Jean Vincent.

Author contributions: Conceptualization: AB, AT, CL, DP, MJP, VF. Formal Analysis: CL, MJP, VF. Funding acquisition: AB, AT, CL, DP, VF. Investigation: JF, FH, LB, MJP, NĐ, VF, AB, MP, RWS, TT Software: CL, VL, MJP. Writing – original draft: AB, MJP. Writing – review & editing: AB, AT, CL, DP, MJP, VF, RWS.

Authors declare that they have no competing interests.

535 **Fig. 1 –Plasticity of $GABA_AR$ in the light/dark cycle is sleep- and microglia-dependent. a**, Experimental
536 groups: mice at dark phase (ZT18), mice at light phase (ZT6) and mice submitted to sleep deprivation
537 (dashed) in the light phase (SD6). Vertical bars: time of perfusion. **b**, Representative images showing
538 enrichment of $GABA_AR\gamma2$ (cyan) at cortical L1 inhibitory synapses in the light phase (ZT6). Arrowheads:
539 $GABA_AR\gamma2$ clusters at $gephyrin^+VGAT^+$ synapses in control (CTL) or PLX3397-treated mice (PLX). Scale
540 bars, 5 and 1 µm. Dashed box corresponds to CTL at ZT18. **c, d,** Mean intensity of $GABA_AR\gamma2$ clusters at
541 $gephyrin^+VGAT^+$ synapses (synaptic) and at extrasynaptic sites normalized to ZT18. n= 48 to 65 fields of
542 view (FOVs) from 4-5 mice per group. *p<0.05, nested t-test; **p<0.01 compared with ZT18 and $^{\#\#}$p<0.01
543 compared with SD6, nested one-way ANOVA followed by Sidak's multiple comparison test. **e**, Left:
544 Representative confocal images of VGAT and $GABA_AR\gamma2$ in cortical L5. Yellow line delineates soma
545 identified by NeuN staining. Scale bar, 5 µm. Right: Mean intensity of $GABA_AR\gamma2$ at somatic $VGAT^+$
546 clusters in L5 normalized to ZT18. n= 60 FOVs from 5 mice per group.
547
548 **Fig. 2 – Microglial P2RX7 -TNFα signaling drives $GABA_ARs$ synaptic enrichment through CaMKIIα**
549 **phosphorylation. a**, Representative confocal images showing increase of $GABA_AR\alpha1$ (cyan) at $gephyrin^+$
550 clusters (arrowheads) upon NMDA-induced inhibitory long-term potentiation (iLTP: 2 min 20 µM
551 NMDA/10 µM CNQX plus 20 min recovery) in organotypic slices cortical L1 (CTL: control; bsl: baseline).
552 **b-e**, Mean intensity of $GABA_AR\alpha1$ clusters at $gephyrin^+$ cluster normalized to CTL at bsl. n= FOVs/
553 independent experiments: (b) n= 44 to 69/ 5 to 6; (c) n= 47 to 53/ 5; (d) n= 66 to 102/ 5 to 7; (e) n= 49 to 68/
554 7 to 9. *p<0.05, **p<0.01 and ***p<0.001, nested one-way ANOVA followed by Sidak's multiple
555 comparison test. iLTP-induced synaptic $GABA_AR$ enrichment is abolished by: **b**, microglia
556 depletion/inactivation (PLX: PLX3397; SAP: Mac1-saporin; minoc: minocycline); **c**, neutralization of TNFα
557 (nTNFα); **d**, microglia-specific TNFα deletion through 4-hydroxy-tamoxifen (4-OHT)-induced
558 recombination on $CX3CR1^{CreERT2/+:}TNF^{f/f}$ but not on a $TNF^{f/f}$ background; **e**, ATP hydrolysis (apy), P2XR
559 antagonist (PPADS) and P2RX7 antagonist (A74), but not P2Y12R inhibitor (PSB). **f**, Left: Confocal images
560 of $GABA_AR\alpha1$ (cyan) at $gephyrin^+$ clusters (arrowheads) in bsl and upon BzATP treatment. Right: Mean
561 intensity of $GABA_AR\alpha1$ clusters at $gephyrin^+$ clusters normalized to CTL at bsl. n= 49 to 63/ 5 to 6. *p<0.05,
562 **p<0.01, nested one-way ANOVA followed by Sidak's multiple comparison test. **g**, Left: Thr286-
563 phosphorylated CaMKII is enhanced in L1 at the induction phase of plasticity (iLTP0' or BzATP0'). Scale
564 bar, 5 µm. Right: Mean intensity of Thr286-phosphorylated CaMKII puncta normalized to bsl. n= 25 to 33
565 FOVs from 3 independent experiments. *p<0.05, nested t-test. **h**, Left: Western blot analysis showing
566 iLTP0'-induced CaMKII Thr286-phosphorylation. Right: Ratio between Thr286-phosphorylated CaMKII
567 and total CaMKII normalized to the respective iLTP-free control. n= 5 to 9 independent experiments.
568 *p<0.05 compared with respective control, Kruskal-Wallis test followed by Dunn's multiple comparisons
569 test. **i**, Model. ATP released downstream NMDA-induced neuronal activity activates microglial P2RX7 with
570 triggers the release of microglial TNFα. TNFα signaling gates CaMKIIα autophosphorylation which controls
571 the enrichment of synaptic $GABA_ARs$ in pyramidal neurons.
572

573 **Fig. 3 – P2RX7 and microglial TNFα promote daily changes in synaptic $GABA_AR$ content and**
574 **CaMKII phosphorylation.** **a**, Representative confocal images of Thr286-phosphorylated CaMKII
575 immunoreactivity in L1 showing higher intensity at ZT6 than ZT18 in transgenic control mice (tCTL). Scale
576 bar, 20 µm. **b**, Mean intensity of Thr286-phosphorylated CaMKII signal in L1 normalized to ZT18 for tCTL,
577 microglia-specific TNFα depletion (micTNFα-KO) and P2rx7-KO mice. n= 37 to 50 FOVs from 4-5 mice
578 per group. **c**, Mean intensity of $GABA_ARγ2$ clusters at $gephyrin^+VGAT^+$ synapses normalized to ZT18. n=
579 48 to 65 FOVs from 4-5 mice per group. *p<0.05 and **p<0.01, nested t-test.
580
581 **Fig. 4 - Microglial TNFα modulates slow waves during NREMS**. **a**, Amounts of vigilance states over 24h
582 reported by 2h segments. Wake, NREMS and REMs are not significantly different between tCTL and
583 micTNFα-KO mice (n=15 mice per group; two-way RM-ANOVA, p=0.1490; p=0.2784, p=0.6838
584 respectively) **b**, Average spectral density (top) of tCTL and micTNFα-KO (lines: means. Shaded area: SEM)
585 and distribution of peak frequency of delta oscillations. The peak delta frequency is significantly lower in
586 micTNFα-KO mice (Mann-Whitney W = 157, p = 0.025). **c**, Left: Examples of EEG and 0.1-4Hz filtered
587 EEG during NREMS from a transgenic control tCTL; the positive and negative peaks of the delta-filtered
588 signal are indicated by orange and blue points, respectively. Ticks on grey lines indicate large positive
589 deflections corresponding to Slow Waves (SW). Right: grand average SW for tCTL(black) showing duration
590 (d) and maximum slope (s), and micTNFα-KO (green). **d**, The micTNFα-KO mice exhibit significantly
591 shorter peak onset slope and longer SW duration than tCTL mice. Mann-Whitney W=42 p=0.005 and
592 W=153, p=0.37 respectively.
593
594 **Fig. 5 – Microglial TNFα required for consolidation of a sleep-dependent motor learning task.** **a**,
595 Experimental design: mice learn to run on the complex wheel (session 1, S1) and consolidation of memory is
596 tested the following day (session 2, S2). Between S1 and S2, mice are left undisturbed in their cages. **b**,
597 Average latency to fall off the complex wheel in the first three and the last three trials of S1 and S2 from
598 tCTL and micTNFα-KO. Grey area represents undisturbed sleep-wake cycle. Dashed line represents S1 to
599 S2 consolidation. **c**, Improvement within each session measured as the ratio between mean of the best three
600 trials and first three trials. **d**, Performance improvement across sessions measured as the ratio between mean
601 of S2 and S1 trials. ***p<0.001, Mann-Whitney test. **e**, Consolidation of motor learning across sessions
602 measured in two ways: ratio between mean of first 3 trials of S2 and mean of last 3 trials of S1 (first S2/ last
603 S1) or ratio between mean of first 3 trials of S2 and mean of S1 trials (first S2/ mean S1). *p<0.05 and
604 **p<0.01, Mann-Whitney test. (b-e) 8 tCTL and 10 micTNFα-KO mice. **f, h,** Novelty preference in the
605 novel floor-texture recognition (FTR) (f) or the Novel Object Recognition (NOR) task (h). Fractional
606 preference is expressed as a function of cumulative time of exploration (see Methods). The data represent the
607 mean+/- sem of the preference for the object placed on the novel floor texture (f) or for the novel object (h)
608 computed for each animal. $^{\#}$p<0.05, $^{\#\#}$p<0.01 and $^{\#\#\#}$p<0.001 preference for one object vs. no preference and
609 *p<0.05, **p<0.01 and ***p<0.001 CTL vs. micTNFα-KO. Unpaired t tests. The fractional preference is
610 equal to 1 or -1 when the animal only explored respectively the object placed on the novel or familiar floor

texture in the FTR and the novel or familiar object in the NOR, and 0 when the animal spent exactly the same amount of time on the two objects. **g, i,** Total duration of exploration of the novel floor (FTR; g) and of the novel object (NOR; i) . Boxes represent quartiles and whiskers correspond to the range of data; points are singled as outliers if they deviate more than 1.5 x inter-quartile range from the nearest quartile. g, °p= 0,0674 CTL vs. micTNFα-KO, Unpaired t tests. **i,** p= 0,44 CTL vs. micTNFα-KO. Unpaired t tests; (f, g) n= 11 tCTL and 8 (f,g) or 16 (h,i) micTNFα-KO mice.

Figure 1

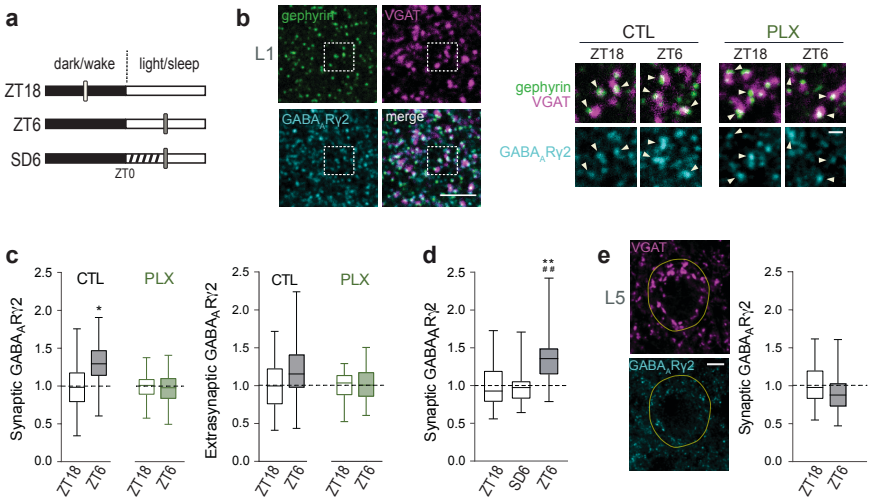

Fig. 1 –Plasticity of GABA$_A$R in the light/dark cycle is sleep- and microglia-dependent. a, Experimental groups: mice at dark phase (ZT18), mice at light phase (ZT6) and mice submitted to sleep deprivation (dashed) in the light phase (SD6). Vertical bars: time of perfusion. **b**, Representative images showing enrichment of GABA$_A$Rγ2 (cyan) at cortical L1 inhibitory synapses in the light phase (ZT6). Arrowheads: GABA$_A$Rγ2 clusters at gephyrin$^+$VGAT$^+$ synapses in control (CTL) or PLX3397-treated mice (PLX). Scale bars, 5 and 1 µm. Dashed box corresponds to CTL at ZT18. **c, d,** Mean intensity of GABA$_A$Rγ2 clusters at gephyrin$^+$VGAT$^+$ synapses (synaptic) and at extrasynaptic sites normalized to ZT18. n= 48 to 65 fields of view (FOVs) from 4-5 mice per group. *p<0.05, nested t-test; **p<0.01 compared with ZT18 and ##p<0.01 compared with SD6, nested one-way ANOVA followed by Sidak's multiple comparison test. **e**, Left: Representative confocal images of VGAT and GABA$_A$Rγ2 in cortical L5. Yellow line delineates soma identified by NeuN staining. Scale bar, 5 µm. Right: Mean intensity of GABA$_A$Rγ2 at somatic VGAT$^+$ clusters in L5 normalized to ZT18. n= 60 FOVs from 5 mice per group.

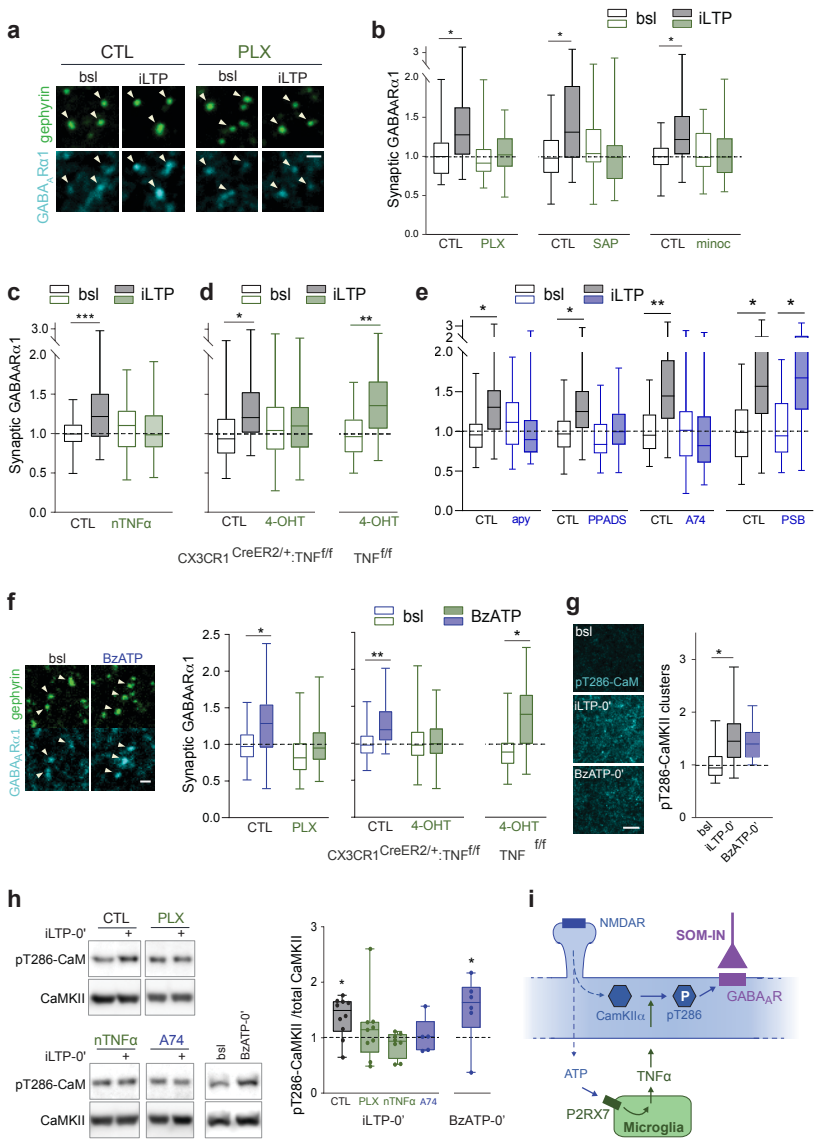

Fig. 2 – Microglial P2X7R-TNFα signaling drives GABA$_A$Rs synaptic enrichment through CaMKIIα phosphorylation. **a**, Representative confocal images showing increase of GABA$_A$Rα1 (cyan) at gephyrin$^+$ clusters (arrowheads) upon NMDA-induced inhibitory long-term potentiation (iLTP: 2 min 20 µM NMDA/10 µM CNQX plus 20 min recovery) in organotypic slices cortical L1 (CTL: control; bsl: baseline). **b-e**, Mean intensity of GABA$_A$Rα1 clusters at gephyrin$^+$ cluster normalized to CTL at bsl. n= FOVs/ independent experiments: (b) n= 44 to 69/ 5 to 6; (c) n= 47 to 53/ 5; (d) n= 66 to 102/ 5 to 7; (e) n= 49 to 68/ 7 to 9. *p<0.05, **p<0.01 and ***p<0.001, nested one-way ANOVA followed by Sidak's multiple comparison test. iLTP-induced synaptic GABA$_A$R enrichment is abolished by: **b**, microglia depletion/inactivation (PLX: PLX3397; SAP: Mac1-saporin; minoc: minocycline); **c**, neutralization of TNFα (nTNFα); **d**, microglia-specific TNFα deletion through 4-hydroxy-tamoxifen (4-OHT)-induced recombination on CX3CR1$^{CreERT2/+}$:TNF$^{f/f}$ but not on a TNF$^{f/f}$ background; **e**, ATP hydrolysis (apy), P2XR antagonist (PPADS) and P2X7R antagonist (A74), but not by P2Y12 antagonist (PSB) **f**, Left: Confocal images of GABA$_A$Rα1 (cyan) at gephyrin$^+$ clusters (arrowheads) in bsl and upon BzATP treatment. Right: Mean intensity of GABA$_A$Rα1 clusters at gephyrin$^+$ clusters normalized to CTL at bsl. n= 49 to 63/ 5 to 6. *p<0.05, **p<0.01, nested one-way ANOVA followed by Sidak's multiple comparison test. **g**, Left: Thr286-phosphorylated CaMKII is enhanced in L1 at the induction phase of plasticity (iLTP0' or BzATP0'). Scale bar, 5 µm. Right: Mean intensity of Thr286-phosphorylated CaMKII puncta normalized to bsl. n= 25 to 33 FOVs from 3 independent experiments. *p<0.05, nested t-test. **h**, Left: Western blot analysis showing iLTP0'-induced CaMKII Thr286-phosphorylation. Right: Ratio between Thr286-phosphorylated CaMKII and total CaMKII normalized to the respective iLTP-free control. n= 5 to 9 independent experiments. *p<0.05 compared with respective control, Kruskal-Wallis test followed by Dunn's multiple comparisons test. **i**, Model. ATP released downstream NMDA-induced neuronal activity activates microglial P2RX7, which triggers the release of microglial TNFα. TNFα signaling gates CaMKIIα autophosphorylation which controls the enrichment of synaptic GABA$_A$Rs in pyramidal neurons.

Figure 3

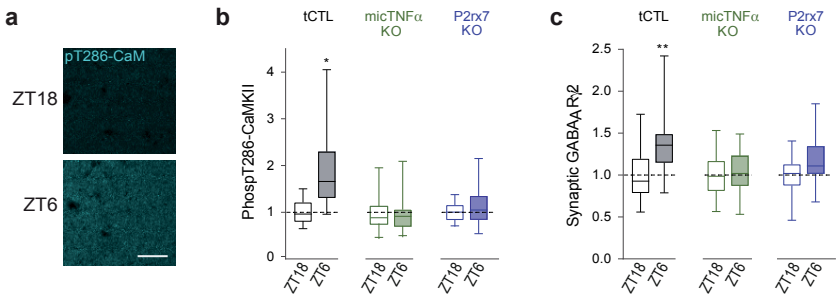

Fig. 3 – P2RX7 and microglial TNFα promote daily changes in synaptic $GABA_AR$ content and CaMKII phosphorylation. a, Representative confocal images of Thr286-phosphorylated CaMKII immunoreactivity in L1 showing higher intensity at ZT6 than ZT18 in transgenic control mice (tCTL). Scale bar, 20 µm. **b**, Mean intensity of Thr286-phosphorylated CaMKII signal in L1 normalized to ZT18 for tCTL, microglia-specific TNFα depletion (micTNFα-KO) and P2rx7-KO mice. n= 37 to 50 FOVs from 4-5 mice per group. **c**, Mean intensity of $GABA_ARγ2$ clusters at $gephyrin^+VGAT^+$ synapses normalized to ZT18. n= 48 to 65 FOVs from 4-5 mice per group. *p<0.05 and **p<0.01, nested t-test.

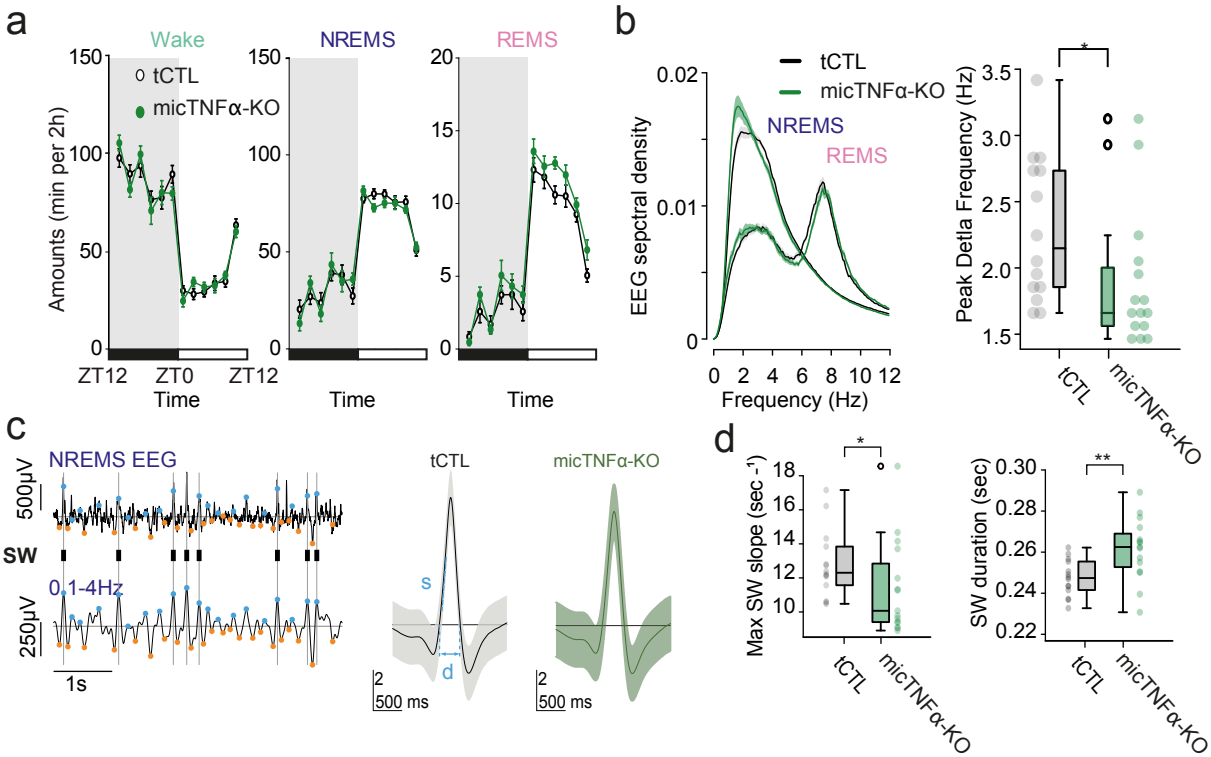

Fig. 4 - **Microglial TNFα modulates slow waves during NREMS**. **a**, Amounts of vigilance states over 24h reported by 2h segments. **b**, Average spectral density (top) of tCTL and micTNFα-KO (lines: means. Shaded area: SEM) and distribution of peak frequency of delta oscillations. The peak delta frequency is significantly lower in micTNFα-KO mice (Mann-Whitney W = 157, p = 0.025). **c**, Left: Examples of EEG and 0.1-4Hz filtered EEG during NREMS from a transgenic control tCTL; the positive and negative peaks of the delta-filtered signal are indicated by orange and blue points, respectively. Ticks on grey lines indicate large positive deflections corresponding to Slow Waves (SW). Right: grand average SW for tCTL(black) showing duration (d) and maximum slope (s), and micTNFα-KO (green). **d**, The micTNFα-KO mice exhibit significantly shorter peak onset slope and longer SW duration than tCTL mice. Mann-Whitney W=42 p=0.005 and W=153, p=0.37 respectively

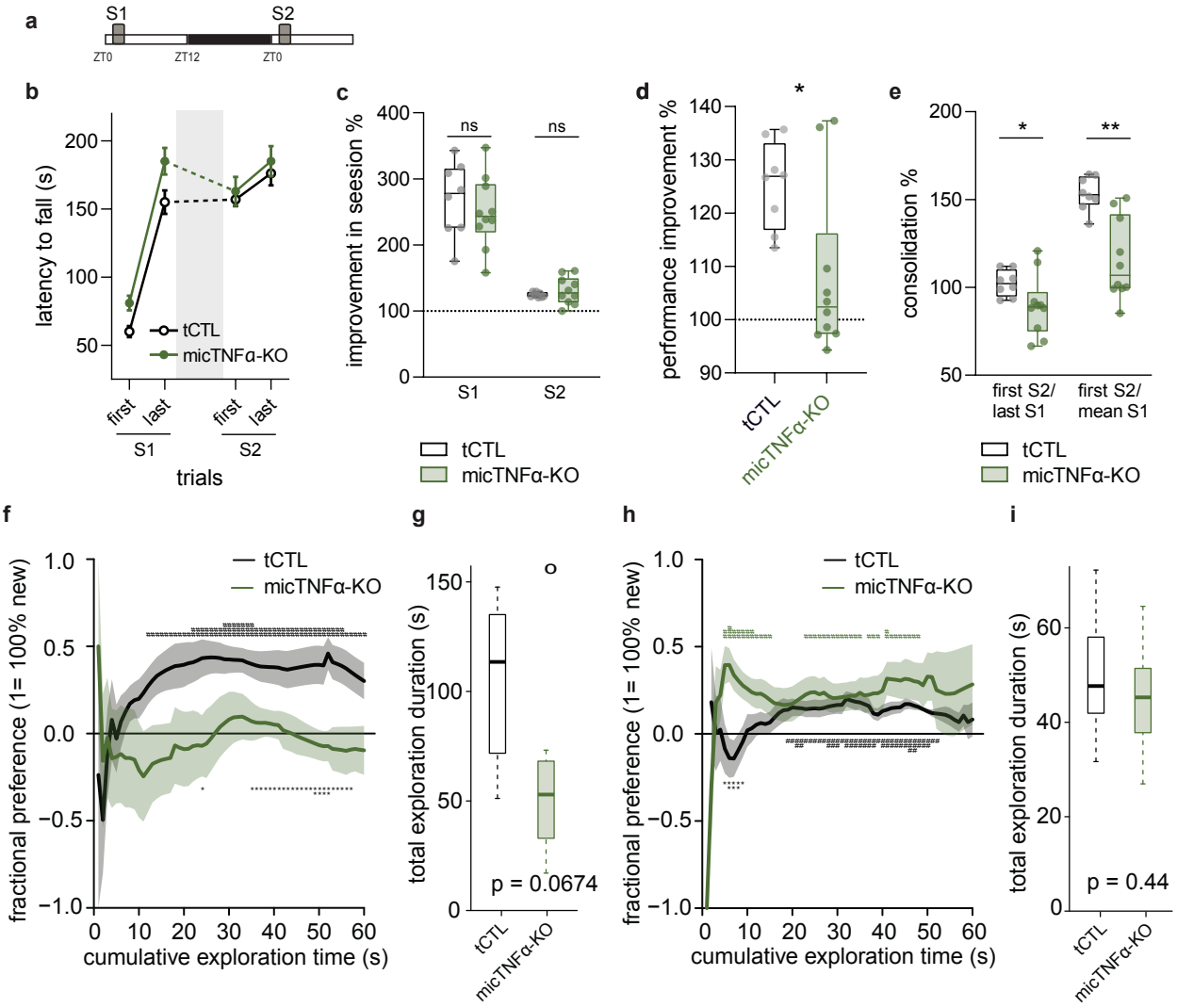

Fig. 5 – Microglial TNFα required for consolidation of a sleep-dependent motor learning task. a, Experimental design: mice learn to run on the complex wheel (session 1, S1) and consolidation of memory is tested the following day (session 2, S2). Between S1 and S2, mice are left undisturbed in their cages. **b**, Average latency to fall off the complex wheel in the first three and the last three trials of S1 and S2 from tCTL and micTNFα-KO. Grey area represents undisturbed sleep-wake cycle. Dashed line represents S1 to S2 consolidation. **c**, Improvement within each session measured as the ratio between mean of the best three trials and first three trials. **d**, Performance improvement across sessions measured as the ratio between mean of S2 and S1 trials. ***p<0.001, Mann-Whitney test. **e**, Consolidation of motor learning across sessions measured in two ways: ratio between mean of first 3 trials of S2 and mean of last 3 trials of S1 (first S2/ last S1) or ratio between mean of first 3 trials of S2 and mean of S1 trials (first S2/ mean S1). *p<0.05 and **p<0.01, Mann-Whitney test. (b-e) 8 tCTL and 10 micTNFα-KO mice. **f, h,** Novelty preference in the novel floor-texture recognition (FTR) (f) or the Novel Object Recognition (NOR) task (h). Fractional preference is expressed as a function of cumulative time of exploration (see Methods). The data represent the mean+/- sem of the preference for the object placed on the novel floor texture (f) or for the novel object (h) computed for each animal. #p<0.05, ##p<0.01 and ###p<0.001 preference for one object vs. no preference and *p<0.05, **p<0.01 and ***p<0.001 CTL vs. micTNFα-KO. Unpaired t tests. The fractional preference is equal to 1 or -1 when the animal only explored respectively the object placed on the novel or familiar floor texture in the FTR and the novel or familiar object in the NOR, and 0 when the animal spent exactly the same amount of time on the two objects. **g, i,** Total duration of exploration of the novel floor (FTR; g) and of the novel object (NOR; i) . Boxes represent quartiles and whiskers correspond to the range of data; points are singled as outliers if they deviate more than 1.5 x inter-quartile range from the nearest quartile. g, °p= 0,0674 CTL vs. micTNFα-KO, Unpaired t tests. **i,** p= 0,44 CTL vs. micTNFα-KO. Unpaired t tests; (f, g) n= 11 tCTL and 8 (f,g) or 16 (h,i) micTNFα-KO mice.

.